Published in final edited form as:

Cell Rep. 2016 August 30; 16(9): 2387–2398. doi:10.1016/j.celrep.2016.07.081.

COX7A2L is a mitochondrial complex III-binding protein that stabilizes the III_2+IV supercomplex without affecting respirasome formation

Rafael Pérez-Pérez[1,2,8], **Teresa Lobo-Jarne**[1,2,8], **Dusanka Milenkovic**[3], **Arnaud Mourier**[3], **Ana Bratic**[3], **Alberto García-Bartolomé**[1,2], **Erika Fernández-Vizarra**[4], **Susana Cadenas**[5,6], **Aitor Delmiro**[1,2], **Inés García-Consuegra**[1,2], **Joaquín Arenas**[1,2], **Miguel A. Martín**[1,2], **Nils-Göran Larsson**[3,7], and **Cristina Ugalde**[1,2,*]

[1]Instituto de Investigación Hospital Universitario 12 de Octubre (i+12), Madrid 28041, Spain

[2]Centro de Investigación Biomédica en Red de Enfermedades Raras (CIBERER), U723, Madrid, Spain

[3]Department of Mitochondrial Biology, Max Planck Institute for Biology of Ageing, 50931 Cologne, Germany

[4]Medical Research Council-Mitochondrial Biology Unit, CB2 0XY Cambridge, UK

[5]Centro de Biología Molecular “Severo Ochoa” (CSIC-UAM) and Departamento de Biología Molecular, Universidad Autónoma de Madrid, 28049 Madrid, Spain

[6]Instituto de Investigación Sanitaria Princesa (IIS-IP), 28006 Madrid, Spain

[7]Department of Medical Biochemistry and Biophysics, Karolinska Institutet, 171 77 Stockholm, Sweden

Summary

Mitochondrial respiratory chain (MRC) complexes I, III and IV associate into a variety of supramolecular structures known as supercomplexes and respirasomes. While COX7A2L was originally described as a supercomplex-specific factor responsible for the dynamic association of complex IV into these structures to adapt MRC function to metabolic variations, this role has been disputed. Here we further examine the functional significance of COX7A2L in the structural organization of the mammalian respiratory chain. As in the mouse, human COX7A2L binds primarily to free mitochondrial complex III and to a minor extent to complex IV to specifically promote the stabilization of the III_2+IV supercomplex without affecting respirasome formation.

*Corresponding author: Dr. Cristina Ugalde, Instituto de Investigación, Hospital Universitario 12 de Octubre, Avenida de Córdoba s/n, 28041 Madrid. Phone: +34 91 779 2784, FAX: +34 91 390 8544, cugalde@h12o.es.

[8]Co-first authors

Author Contributions: Conceptualization, Methodology and Investigation, R.P.P., T.L.J., D.M., A.M., A.B., A.G.B., E.F.V., I.G.C., and C.U.; Formal Analysis, A.D.; Writing, C.U.; Funding Acquisition, S.C., E.F.V., M.A.M., N.G.L., and C.U.; Resources, E.F.V., J.A., and N.G.L.; Supervision, S.C., N.G.L., and C.U.

Furthermore, COX7A2L does not affect the biogenesis, stabilization and function of the individual OXPHOS complexes. These data show that independent regulatory mechanisms for the biogenesis and turnover of different MRC supercomplex structures co-exist.

Graphical abstract

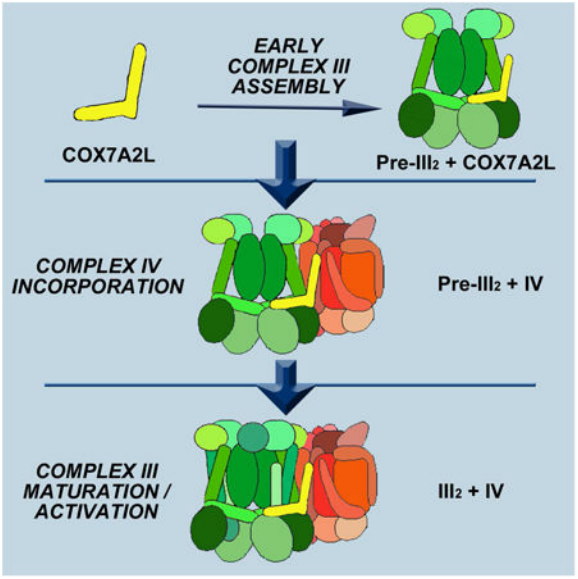

Introduction

The oxidative phosphorylation (OXPHOS) system is embedded in the lipid bilayer of the inner mitochondrial membrane and is composed of five multiprotein enzyme complexes as well as the two mobile electron carriers coenzyme Q (or Q) and cytochrome *c* (cyt *c*). The first four enzyme complexes (CI-CIV) comprise the mitochondrial respiratory chain (MRC), which facilitates electron transfer from reducing equivalents to molecular oxygen. The electron translocation through the MRC is coupled to the creation of a proton gradient across the inner mitochondrial membrane that will be used by the ATP synthase (complex V) to drive ATP synthesis. In recent years, it has been widely demonstrated that MRC complexes I, III and IV (CI, CIII, CIV) may associate to form a diversity of supramolecular assemblies known as supercomplexes (SCs) or respirasomes (Cruciat et al., 2000; Schagger and Pfeiffer, 2000). However, the functional relevance of mitochondrial SCs is a matter of intense debate though they are conserved across species. In mammals, the respirasome is often referred to as SC I+III_2+IV_{1-4}. Biochemical analyses support the idea that the respirasome contains the MRC and the electron carriers and thus is a structural entity that can carry out respiration on its own (Acin-Perez et al., 2008). Some authors have proposed that SCs function to confer stability to CI (Moreno-Lastres et al., 2012; Schagger et al., 2004), to reduce reactive oxygen species (ROS) production (Maranzana et al., 2013), to facilitate electron channeling (Bianchi et al., 2004) and to mediate metabolic adaptation through the partition of Q into two different pools (Lapuente-Brun et al., 2013). However, the view that SC assemblies provide distinct electron translocation pathways is currently disputed. Kinetic and spectroscopic studies have challenged the substrate channeling model by concluding that (i)

cyt *c* is not trapped within the SCs and therefore it does not encounter any restriction of its diffusion (Trouillard et al., 2011), and (ii) the metabolic pathways for NADH and succinate oxidation impose different coenzyme Q redox steady state but communicate and converge on a single non-partitioned coenzyme Q pool (Blaza et al., 2014; Rigoulet et al., 2010). Moreover, cryo-electron microscopy analyses of the mammalian SC $I+III_2+IV_1$ does not support the substrate channeling model because the distance between the binding sites for coenzyme Q on CI and CIII, as well as the distance between the binding sites for cyt *c* on CIII and CIV, are sufficiently far away to allow free exchange (Althoff et al., 2011; Dudkina et al., 2011). Instead, it has been suggested that the relatively weak interactions between the MRC complexes that lead to SCs formation, could prevent deleterious protein aggregation in the densely packed inner mitochondrial membrane (Blaza et al., 2014). According to this latter idea, SCs formation would have no direct bioenergetic role but rather be a protective mechanism that prevents tight interactions between the individual OXPHOS complexes.

In budding yeast lacking CI, the formation and stabilization of the mitochondrial SC III_2+IV_{1-2} is controlled by specific regulatory proteins called the respiratory supercomplex factors 1 and 2 (Rcf1 and Rcf2) (Chen et al., 2012; Strogolova et al., 2012; Vukotic et al., 2012). While both proteins are preferentially associated with CIV, only Rcf1 seems to play a crucial role in SC stability, as it does its human ortholog HIG2A (Chen et al., 2012). A highly controversial issue involves the potential regulatory role of the protein COX7A2L/COX7RP in the formation and stabilization of mitochondrial SCs. Mouse COX7A2L was reported to be present in SC III_2+IV and the respirasomes, but not in free complex III or IV (Lapuente-Brun et al., 2013; Müller et al., 2015), and was therefore renamed the SC-specific assembly factor I (SCAFI). Certain wild-type mouse strains, e.g. C57BL/6J and BALB/c, are homozygous for a 6 bp deletion in the *Cox7a2l* gene and therefore express a short, unstable COX7A2L variant that was reported to lead to a failure to form SC III_2+IV and respirasomes (Lapuente-Brun et al., 2013). Remarkably, the respiration rates and ATP production from CI and CII-linked substrates were reported to be higher in tissues from mice bearing the short COX7A2L isoform. The authors suggested that COX7A2L could mediate binding of CIV to SCs to physiologically regulate energy metabolism by providing alternate paths for electrons from different metabolic sources (NADH, FAD, or both), thus allowing optimization of respiration to substrate availability (for discussion, see (Barrientos and Ugalde, 2013)). Another study used *Cox7a2l* knockout mice (Ikeda et al., 2013) and reported that COX7A2L is a SC-specific factor that, in contrast to the previous model (Lapuente-Brun et al., 2013), would promote respirasome stability to gain full activity of the MRC. The knockout study showed that respirasomes were present in mitochondria from skeletal muscle of C57BL/6J mice (Ikeda et al., 2013), despite previous claims that this mouse strain lacks respirasomes (Lapuente-Brun et al., 2013). In agreement, an in depth characterization of isolated heart and liver mitochondria from control mouse strains that either contained the full-length *Cox7a2l* gene (i.e., CD1 mice) or the variant with the 6 bp deletion (i.e., C57BL/6J, C57BL/6N and BALB/c mice), demonstrated that all mice had normal formation of respirasomes and normal respiratory chain function, thus showing that the truncated version of the *Cox7a2l* gene does not impact the bioenergetic capacity *in vivo* (Mourier et al., 2014a).

The aim of the present work was to elucidate the functional importance of COX7A2L in the structural organization of the mammalian OXPHOS system. Our study demonstrates that COX7A2L preferentially interacts with mitochondrial CIII and to a minor extent with CIV to promote stabilization of the SC III_2+IV in both mice and humans. However, COX7A2L has no role in the biogenesis, stabilization and function of the free OXPHOS complexes and it has no role in the formation of the respirasomes. These data show the co-existence of alternative regulatory mechanisms for the biogenesis and turnover of different respiratory chain SC structures.

Results

Mouse COX7A2L is essential for SC III_2+IV formation in a respirasome-independent manner

In order to shed light on these contradictory conclusions regarding COX7A2L function in murine models (Ikeda et al., 2013; Lapuente-Brun et al., 2013; Mourier et al., 2014a), we first analyzed the COX7A2L levels relative to OXPHOS subunits by western blots in isolated heart mitochondria from CD1 versus C57BL/6 mice (Figure S1A). The allelic variation of the *Cox7a2l* gene in nuclear DNA is previously described (Mourier et al., 2014a). The CD1 mice express high levels of a 113 amino acid COX7A2L protein isoform, whereas C57BL/6 mice express low levels of a slightly shorter and unstable COX7A2L protein isoform of 111 amino acids. CI and CIV subunits were present at similar levels in the wild-type CD1, C57BL/6J and C57BL/6N mice strains. However, the levels of COX7A2L and CIII subunits were slightly increased in the CIV-deficient conditional *Lrpprc* knockout mice compared with their wild-type littermates that all were maintained on the C57BL/6N background (Mourier et al., 2014b). These data suggest that COX7A2L as well as CIII are stabilized in the *Lrpprc* knockout mice as a response to the severe CIV deficiency.

In agreement with a previous report (Mourier et al., 2014a), BN-PAGE analysis of digitonin-solubilized heart mitochondria from CD1 and C57BL/6 mice confirmed similar levels and activities of the respirasomes in all wild-type strains (Figures 1A-B). Analysis of COX7A2L distribution in CD1 mice (Figure 1C) showed its preferential co-segregation with free CIV, SC III_2+IV and respirasomes, and to a minor extent with the CIII dimer. In the C57BL/6 mice, however, COX7A2L was mostly found in CIII-containing structures (Figure 1C). These data suggest that the two-amino acid deletion and consequent reduction in COX7A2L levels mostly hampers the binding of COX7A2L to CIV, which nevertheless only provoked the disappearance of SC III_2+IV (Figures 1B-C), without affecting free CIV or respirasome levels and activities (Figures 1A-C). Thus, the severely reduced COX7A2L levels in C57BL/6 mice do not hamper the association of CIV with the respirasomes, as previously proposed (Lapuente-Brun et al., 2013). To test whether the respirasome stability depends on COX7A2L levels, we exposed heart mitochondria from CD1 and C57BL/6J mice to increasing amounts of the detergent digitonin followed by BN-PAGE analysis (Figure S1B). Respirasome levels and organization were comparable between both mouse strains at the low digitonin-to-protein ratios. Also under the most stringent detergent conditions, respirasomes were still clearly detectable in the C57BL/6J mice albeit at slightly lower levels than in the CD1 mice. Noteworthy, SCs from both mouse strains reorganized in

different ways upon increasing digitonin treatment and some respirasome bands appeared to be more stable in C57BL/6J than in CD1 mice, and vice versa. We next analyzed DDM-solubilized mouse heart mitochondria, condition in which respirasomes are disrupted (Figure S1C), and found that the co-segregation between COX7A2L and free CIV was totally lost, suggesting that their interaction is indeed labile. In CD1 mice, both COX7A2L and the CIII subunit CORE2 co-localized with the CIII dimer and SC III_2+IV, whereas in C57BL/6 mice both proteins only were present in the CIII dimer. These data show that COX7A2L is essential for SC III_2+IV stability, whereas it is dispensable for the respirasome formation.

Next we assessed import and assembly of the radiolabeled 113 amino acid COX7A2L isoform into isolated heart mitochondria from CD1, C57BL/6J and C57BL/6N mice by BN-PAGE analyses (Figures 1D and S1D-E). We used mitochondria with dissipated membrane potential as controls to ensure that the protein import and assembly depends on the membrane potential across the inner mitochondrial membrane (Figure S1D). The comparison of migration patterns and the kinetics of formed assembly intermediates after import of COX7A2L or the CIII subunit RISP showed that the long COX7A2L isoform was incorporated into CIII-containing structures in all mice strains. We observed a preferential co-segregation of the newly imported COX7A2L with the CIII dimer at early time points after import (Figure 1D), whereas COX7A2L was present in higher molecular weight structures, such as SC III_2+V and respirasomes, at later time points. These data demonstrate that COX7A2L preferentially interacts with CIII prior to SC formation. Additional import analyses of COX7A2L into isolated mitochondria from *Lrpprc* wild-type and knockout hearts (Figure S1E) revealed that COX7A2L associates with CIII independently of the presence of CIV.

Human COX7A2L co-localizes with respiratory chain complexes III and IV, and complex III-containing supercomplexes

In humans, only one COX7A2L protein of 114 amino acids has been reported in the NCBI database (http://www.ncbi.nlm.nih.gov/gene/9167). To clarify the functional role of the human COX7A2L protein, we first analyzed its distribution pattern in relation to free MRC complexes and SCs by performing BN-PAGE followed by western blot analyses. We analyzed digitonin-solubilized mitochondria from control 143B cells and cybrids with a severe CI assembly defect (CI-KD), total lack of CIII (CIII-KO) or total lack of CIV (CIV-KO) (Figures 2A and S2A). In controls, COX7A2L co-localized not only with SC III_2+IV and the respirasomes (SC I+III_2+IV_n), as previously described in murine models (Lapuente-Brun et al., 2013; Müller et al., 2015), but also with SC I+III_2, the CIII dimer ($CIII_2$) and free CIV. The CI-KD cybrids, which harbored a >90% heteroplasmic mutation in the *MT-ND2* subunit gene of mtDNA (Ugalde et al., 2007), showed a strong reduction in the levels of SC I+III_2+IV_n, SC III_2+IV and free CIV. Consistently, the amounts of COX7A2L within those structures were also reduced in the CI-defective cells compared with the controls. The CIII-KO cybrids lacked CIII due to a homoplasmic 4–base pair deletion in the *MT-CYB* gene that encodes cytochrome *b* (Rana et al., 2000). Lack of CIII caused the complete disruption of SC I+III_2+IV_n and SC III_2+IV accompanied by increased levels of free CIV and CIV oligomers. In addition, a dramatic reduction in COX7A2L levels, comparable to that of the CIII structural subunits, was observed (Figure 2B). Only a minor residual

COX7A2L signal co-migrating with free CIV was seen at the longest exposures (Figure S2B), indicating that the lack of CIII profoundly affects the stability of COX7A2L and its binding to CIV. The CIV-KO cybrids harbor a homoplasmic nonsense mutation in *MT-CO1* (Bruno et al., 1999), leading to the disappearance of free CIV, SC III_2+IV and SC I +III_2+IV_n, accompanied by an accumulation of SC I+III_2 and $CIII_2$. Interestingly, COX7A2L could bind SC I+III_2 and $CIII_2$ in the absence of CIV, whereas very small amounts were bound to CIV in the absence of CIII. Thus, in human cells COX7A2L preferentially associates with $CIII_2$ and CIII-containing structures and only to a minor extent with free CIV, showing that COX7A2L principally behaves as a CIII interactor rather than an assembly factor exclusive to CIV-containing SCs (Lapuente-Brun et al., 2013). The presence of COX7A2L in $CIII_2$, SC I+III_2 and I+III_2+IV_n was further confirmed by high-resolution nano-LC/ESI-MS proteomic analysis of the blue native gel bands corresponding to SC I+III_2+IV_n in 143B cells, and to SC I+III_2 and $CIII_2$ in the CIV-KO mutant cybrids (Figures 2C-D and Table S1).

Overexpressed COX7A2L is imported into mitochondria and binds complexes III and IV without significantly enhancing supercomplex formation

We next investigated the cellular localization of human COX7A2L by transfecting control 143B cells with a construct expressing COX7A2L with a C-terminal GFP-tag, of~ 39.3 kDa (Figure S3A). Confocal microscopy showed co-localization of COX7A2L-GFP with the ATP synthase (complex V), thus confirming mitochondrial localization of the fusion protein (Figure 3A). Next, we analyzed by BN-PAGE the mitochondrial distribution of exogenous COX7A2L and the effect of *COX7A2L* overexpression on the assembly of the OXPHOS system. To this end, we initially used 143B cells transfected either with the GFP-tagged COX7A2L construct or with a vector that expressed COX7A2L with a C-terminal MYC-DDK-tag, of~ 16.2 kDa (Figures 3B and S3B). In 143B cells, COX7A2L-GFP was effectively overexpressed by~ 15-fold relative to the endogenous COX7A2L (Figure S3A), while COX7A2L-MYC-DDK was overexpressed by~ 2-fold (Figure S3B). BN-PAGE analyses confirmed the co-migration of exogenous COX7A2L with the CIII dimer, free CIV, SC III_2+IV and with the respirasomes in digitonin-solubilized mitochondria (Figures 3B and S3C), thus showing that COX7A2L with both tags are efficiently incorporated into MRC complexes and SCs. Densitometric analyses of OXPHOS subunit distribution showed that the overexpression of tagged-COX7A2L induced no significant increase in the amounts of CIII- and CIV-containing structures (Figure 3C). We extended this analysis to HEK293 cells transfected with either the MYC-DDK-tagged COX7A2L construct or the MYC-DDK tag alone. In HEK293 cells, COX7A2L-MYC-DDK was effectively overexpressed by~ 10-fold relative to endogenous COX7A2L (Figure S3B), and co-migrated with the CIII dimer, free CIV, SC III_2+IV and the respirasomes (Figure S3D). Tagged-COX7A2L overexpression in HEK293 cells neither altered the levels of MRC complexes or SCs.

Next, we tested whether the COX7A2L co-localization with MRC complexes III and IV was due to a direct physical interaction. We performed co-immunoprecipitation assays of digitonin-solubilized mitochondrial lysates from HEK293 cells transfected with either the COX7A2L-MYC-DDK construct or the empty vector (Figure 4A). Immunoprecipitation with an anti-DDK antibody specifically pulled down the tagged-COX7A2L protein in cells

overexpressing COX7A2L-MYC-DDK. In addition, the CIII subunits CORE1, CORE2, CYC1, RISP and UQCRQ, and the CIV subunits COX1, COX4, COX5B and COX6C were detected in the co-immunoprecipitate (co-IP). The CI subunits NDUFA9 and NDUFS1 were barely detectable and CII was not detected in the co-IP samples. When reverse immunoprecipitation assays were performed using antibodies against CORE2 or COX1 proteins, both the tagged and the endogenous COX7A2L proteins were successfully pulled down (Figures 4B-C). Importantly, immunoprecipitation with CORE2 (but not with COX1) pulled down the endogenous COX7A2L protein in cells transfected with the empty vector. These data show that COX7A2L physically interacts with complexes III and IV, but presents a higher affinity for CIII. According to the TOPCONS prediction software (http://topcons.cbr.su.se/), human COX7A2L contains one transmembrane domain that spans amino acids 86 to 107, leaving most of the N-terminal part of the protein exposed to the mitochondrial matrix, and a short C-terminal stretch of 7 amino acids facing the inter membrane space. The direct association of COX7A2L with mitochondrial complexes III and IV is therefore compatible with its predicted topology.

Endogenous COX7A2L associates with respiratory chain complexes III and IV and with supercomplexes during their assembly process

We next analyzed the assembly kinetics of COX7A2L into MRC complexes and SCs by doxycycline-induced reversible inhibition of mitochondrial translation in control 143B cells (Moreno-Lastres et al., 2012). Doxycycline was removed from cell culture media after 6 days of treatment, and samples were collected at different time points (0, 6, 15, 24, 48, 72 and 96 hours). To follow the integration of endogenous COX7A2L into newly-assembled CIII, CIV and SCs, digitonin-solubilized mitochondria were separated by 2D-BN/SDS-PAGE and subsequently analyzed by western blot using antibodies that recognize COX7A2L, CORE2 (CIII), RISP (CIII) and COX5A (CIV) (Figure 5A). Signals from at least three independent experiments were quantified by densitometry, normalized to CII levels and values were expressed relative to levels in untreated cells (SS, Figures 5B-C and S4A-D). After 6 days of doxycycline treatment (time 0h), there was a drastic decrease (80-95%) in the levels of the CIII dimer ($CIII_2$), CIV, SC III_2+IV and SC I+III_2+IV_n, as well as in the levels of COX7A2L that co-localizes with these structures. The CII levels remained normal after doxycycline treatment (not shown) as expected because this complex lacks mtDNA-encoded subunits. Once mitochondrial translation resumed (times 6-96 h, Figures 5B-C), we observed a gradual increase of the levels of COX7A2L protein that co-localized with $CIII_2$, in agreement with our previous results showing co-localization of newly-imported COX7A2L and the CIII dimer in mouse heart mitochondria (Figure 1D). The incorporation of COX7A2L into CIII occurred in parallel to the insertion of the CORE2 subunit, which gets assembled into CIII prior to the incorporation of RISP (Figure S4A). In contrast, the CIV levels increased prior to the binding of COX7A2L (Figure S4B), suggesting that COX7A2L only binds fully-assembled CIV. Once COX7A2L had bound to CIV, there was a simultaneous increase of the levels of COX7A2L in CIV and SC III_2+IV (Figures 5B-C). Moreover, COX7A2L was incorporated into SC III_2+IV in parallel with the CORE2 and COX5A subunits, but prior to the integration of RISP in this structure (Figure S4C). The incorporation of COX7A2L into respirasomes occurred concomitantly with the integration of CORE2 and COX5A, and earlier than the integration of RISP (Figure S4D),

which indicates that COX7A2L is incorporated before the respirasome formation is completed.

COX7A2L associates with complex III and supercomplex III_2+IV prior to the insertion of the RISP catalytic subunit

In the reported CIII assembly models, incorporation of CORE2 allows the formation of a non-functional intermediate called pre-CIII, which contains CORE2 and the rest of CIII subunits except RISP and the smallest subunit (Qcr10 in yeast, UQCR11 in mammals), which are incorporated at a later assembly stage (Fernandez-Vizarra and Zeviani, 2015; Smith et al., 2012). This late assembly step is promoted by LYRM7/MZM1L, an assembly factor that binds RISP to stabilize it prior to its incorporation into CIII. HeLa cells that stably overexpress HA-tagged MZM1L show sequestering of RISP in a small subcomplex, thereby preventing CIII maturation (Sánchez et al., 2013). Doxycycline experiments suggested that human COX7A2L could be a component of pre-CIII, as this protein gets incorporated into CIII in parallel with the CORE2 subunit but before the incorporation of RISP (Figure S4A). To confirm this hypothesis, we analyzed COX7A2L distribution by BN-PAGE of digitonin-solubilized mitochondria isolated from HeLa cells overexpressing MZM1L-HA (Figure 6). As observed by CI *in gel* activity (IGA), MZM1L over expression induced a decrease in the levels and activity of the respirasomes (SC I+III_2+IV), as well as an accumulation of CI-containing structures (Figure 6A). As expected, the levels of the RISP subunit were strongly decreased in the respirasomes, SC III_2+IV and in the CIII dimer, and there was a parallel accumulation of RISP in a small subcomplex that also contains MZM1L-HA (Sánchez et al., 2013) (Figure 6B). The amount of RISP remained relatively high in SC I+III_2+IV compared with other structures, suggesting that this subunit is stably bound to the respirasomes. Upon MZM1L/LYRM7 overexpression, CORE2 and COX7A2L co-segregated with pre-SC III_2+IV and pre-CIII (Figure 6B), further supporting that COX7A2L associates with pre-CIII before the incorporation of RISP takes place (Figure S4E). All in all, our data demonstrate that in human cells, the interaction of COX7A2L with CIV depends on the presence of pre-CIII, which formation is not affected by the lack of RISP (Figure 6) but is dependent on cytochrome *b* (Figure 2B).

COX7A2L downregulation causes supercomplex III_2+IV disassembly without altering respirasome stability or respiratory chain function

We further investigated the effect of *COX7A2L* knockdown on mitochondrial function by using a mix of two small interfering RNAs (siRNAs) targeting exons 2 and 3 of *COX7A2L* mRNA. The *COX7A2L* knockdown efficiency was analyzed by SDS-PAGE of whole cell protein extracts from control 143B cells and CIV-KO mutant cybrids (Figures S5A-B). *COX7A2L* RNAi effectively knocked down the COX7A2L protein by 80% in the 143B cells and by 74% in the CIV-KO mutants, compared with cells transfected with unspecific scrambled siRNAs (C-). Next we analyzed the effects of *COX7A2L* silencing on OXPHOS system assembly by BN-PAGE in combination with CI *in-gel* activity and Western-blot analyses of mitochondrial-enriched fractions from 143B and CIV-KO cells (Figure 7A). Upon *COX7A2L* knockdown, there was a significant decrease in the signals of COX7A2L that co-localized with the CIII dimer, free CIV, and SCs III_2+IV, I+III_2 and I+III_2+IV_n. Despite the severe drop in COX7A2L levels we only observed a specific reduction in the

levels of SC III_2+IV in the 143B cells, whereas the CI activity as well as levels of free OXPHOS complexes, other SCs and respirasomes were normal.

To gain deeper insight into the nature of SC III_2+IV disruption in 143B cells, we performed 2D-BN/SDS-PAGE and western blot analyses with antibodies against CORE2 (CIII), RISP (CIII), COX1 (CIV) and COX5B (CIV) (Figure 7B). Quantification of results from five independent experiments (Figures 7C and S5C-D) showed that *COX7A2L* knockdown specifically led to a significant decrease in the levels of the four analyzed subunits within SC III_2+IV, but not in the other CIII- and CIV- containing structures. These data indicate that COX7A2L has a specific role in the stabilization of SC III_2+IV, but not in the respirasome maintenance. Moreover, *COX7A2L* silencing did not result in a clear accumulation of intermediates smaller than complexes III and IV, indicating that their assembly and/or stability are not disturbed. In agreement with these results, *COX7A2L* knockdown in the CIV-KO mutant cybrids produced no significant alterations in the levels of the CIII dimer or SC I+III_2 (Figures S6A-B). Altogether, our results show that the stabilization of SC III_2+IV relies on the association of COX7A2L with MRC complexes III and IV.

Finally, we measured oxygen consumption rates (OCR) in 143B cells and found no significant differences between *COX7A2L*-silenced cells and cells transfected with scrambled siRNA (Figure S6C). In contrast, mitochondrial respiration was drastically reduced in the CI-KD cybrids that retained SC III_2+IV but showed minimal levels of CI and respirasomes (Figure S6D). Respiratory chain activities measured in *COX7A2L*-silenced 143B cells were also comparable to the activities in control cells (Figure S6E). These results show that a substantial loss of COX7A2L and SC III_2+IV has no significant impact on MRC function in human cell lines.

Discussion

We have investigated the role of COX7A2L/COX7RP in the structural organization of the mammalian OXPHOS system, and clarified the apparent contradictions about the role of this protein in the literature (Ikeda et al., 2013; Lapuente-Brun et al., 2013; Mourier et al., 2014a). Our data demonstrate that COX7A2L acts as a CIII-binding protein in mitochondria from mouse heart and human cell lines. Furthermore, COX7A2L is specifically required for SC III_2+IV maintenance and this finding strongly argue against its previously proposed function as a SC-specific assembly factor that mediates respirasome formation.

We used a combination of COX7A2L immunodetection, high-throughput proteomics and mitochondrial *in vitro* import assays to demonstrate that COX7A2L co-migrates with the CIII dimer, free CIV, SC I+III_2+IV_n, SC I+III_2 and SC III_2+IV in both mice and humans. Thus, the COX7A2L protein is not exclusively present in SCs, as previously reported (Lapuente-Brun et al., 2013; Müller et al., 2015), but instead it predominantly associates with different CIII-containing structures. In mice, the long COX7A2L isoform preferentially interacts with CIII prior to SC formation. The small amount of COX7A2L that co-segregates with free CIV in the CD1 strain could reflect continuous turnover and exchange cycles between the SC-bound and free CIV states, or alternatively, a fraction of the COX7A2L-bound CIV could be dissociated from SCs upon detergent extraction. Such dissociation

cannot be observed in the C57BL/6 mice because they have already lost the association between COX7A2L and CIV. Our data in human control and mutant cybrids lacking one MRC complex suggest that COX7A2L behaves as a structural component of CIII because COX7A2L preferentially binds this complex and the stability of COX7A2L depends on the presence of CIII. Accordingly, COX7A2L remains associated with the CIII dimer and CIII-containing SCs in the absence of complexes I and IV. Furthermore, COX7A2L binds to a reported CIII assembly intermediate that lacks the RISP subunit (pre-CIII) before it interacts with free CIV, SC III_2+IV or the respirasomes. In agreement with this observation, COX7A2L remained associated with pre-CIII in HeLa cells with an impaired incorporation of RISP. In contrast, lack of cytochrome *b* precludes the formation of pre-CIII and led to the disappearance of CIV-associated COX7A2L.

At variance with previous studies in fibroblasts from COX7A2L deprived mice (Lapuente-Brun et al., 2013), COX7A2L overexpression in human cell lines did not cause a significant increase in the levels of MRC complexes III, IV or SCs. However, reduced COX7A2L levels led to a specific loss of SC III_2+IV, but did not affect the amounts of free complexes III and IV, respirasomes or mitochondrial function. Similar to the situation in cultured human cells, the mouse COX7A2L variant of 113 amino acids is imported into mitochondria, where it preferentially associates with CIII-containing structures and plays an essential role in SC III_2+IV stabilization. These results show that mammalian COX7A2L is essential to maintain SC III_2+IV stability, but it plays no critical role in the assembly or stabilization of SC I $+III_2+IV_n$. These findings strongly suggest that there are independent regulatory mechanisms for the biogenesis and turnover of SC III_2+IV and the respirasomes. This is in accordance with previous observations suggesting that SC III_2+IV gets fully-assembled after the completion of respirasome formation (Moreno-Lastres et al., 2012). Our current results also confirm that the levels of respirasomes and MRC activities in mitochondria from mouse hearts are not dependent on the allelic variations of *Cox7a2l* (Mourier et al., 2014a), and contradict the hypothesis that COX7A2L is an assembly factor that regulates respirasome formation to modulate respiration. The fact that respirasomes (but not SC III_2+IV) are present in C57BL/6J mitochondria solubilized with a variety of detergent concentrations provides additional support for a role for COX7A2L to stabilize SC III_2+IV. These data are in agreement with previous reports that show the presence of respirasomes in different tissues, including heart, liver and skeletal muscle, of C57BL/6 mice (Hatle et al., 2013; Ikeda et al., 2013; Jha et al., 2016; Milenkovic et al., 2013). In this regard, the previously reported absence of respirasomes in mouse strains with the truncated *Cox7a2l* allele (Lapuente-Brun et al., 2013) could have resulted from differences in the methodologies or reagents used for membrane solubilization. Indeed, we observed some variations in the intensity of SC isoforms between C57BL/6J and CD1 mice at high detergent concentrations; however the pattern was not constant, as specific SCs were stabilized in C57BL/6J mice but not in CD1 mice and vice versa. Based on our data we cannot exclude the possibility that the mechanisms of SC assembly are regulated in a tissue-dependent manner as recently proposed (Jha et al., 2016). However, it is important to acknowledge that the observed changes may not necessarily be a consequence of genetic COX7A2L variation, but could well be explained by other types of genetic differences among mouse strains.

Our results argue that COX7A2L is permanently associated with CIII and that it exists in association/dissociation equilibrium with CIV, which can define the fate of CIV depending on whether COX7A2L is bound or not. This could provide a mechanism whereby COX7A2L-bound CIV is guided to the proximity of CIII to form and stabilize SC III_2+IV_n. The functional role of COX7A2L may resemble that described for HIG2A, the human ortholog of the yeast Rcf1 SC factor. In yeast, Rcf1 and Rcf2 preferentially associate with CIV to mediate SC III_2+IV_{1-2} stability (Chen et al., 2012; Strogolova et al., 2012; Vukotic et al., 2012). Whereas Rcf2 is yeast-specific, several human homologs of Rcf1 have been reported, whereof HIG2A is involved in the stabilization of a proportion of CIV-containing SCs (Chen et al., 2012). C11ORF83 or UQCC3A, a cardiolipin-binding protein involved in early stages of human CIII assembly, has also been reported to act as a SC III_2+IV stabilizing factor (Desmurs et al., 2015). The similarities in modes of action between these proteins and COX7A2L make it conceivable that they could act in conjunction having a respiratory chain “stabilizing” or “gluing” function, although further studies are required to demonstrate such functional interactions.

Interestingly, the COX7A2L-mediated absence of SC III_2+IV_n does not affect respirasome formation or maintenance. In addition, the fact that the formation and stabilization of a less abundant structure such as SC III_2+IV_n is regulated by specific proteins in a respirasome-independent manner supports the existence of alternative assembly pathways for SC III_2+IV_n and the respirasomes. It may also be indicative of a specific, yet not well understood, physiological importance of SC III_2+IV_n. Results from others have suggested that SC III_2+IV_n could provide a MRC structure to receive electrons from CII (Lapuente-Brun et al., 2013). However, given current evidence that puts in doubt the catalytic roles for mitochondrial SCs (Blaza et al., 2014; Trouillard et al., 2011), alternative non-catalytic functions should also be considered. These would include the regulation of MRC complexes distribution in specific cardiolipin microdomains within the densely protein-packed mitochondrial inner membrane, or a role in storage or preservation of excess MRC components to avoid futile continuous cycles of turnover and *de novo* synthesis. The experimental evidence of independent regulatory mechanisms and proteins for the biogenesis of intermediate SCs and the respirasomes opens new doors for exciting future investigations of the role for these supramolecular structures in the regulation of cellular energy supply.

Experimental Procedures

Cell Cultures

The CI-deficient cell line (CI-KD) harbors a homoplasmic m.4681T>C mutation in the *MT-ND2* subunit gene that leads to a severe CI assembly defect due to a p.L71P substitution (Ugalde et al., 2007). The CIII mutant (CIII-KO) cell line contains a homoplasmic 4–base pair deletion in the *MT-CYB* gene affecting the *de novo* synthesis of cytochrome *b* (Rana et al., 2000). The CIV mutant cell line (CIV-KO) lacks holo-COX due to the homoplasmic m. 6930G>A transition in the *MT-COI* gene, which creates a stop codon that results in a predicted loss of the last 170 amino acids of the COX1 polypeptide (Bruno et al., 1999). HeLa cells, either transduced with the empty pWPXLd-ires-PuroR vector or overexpressing

LYRM7-001-HA (MZM1L-HA), were generated as previously described (Sanchez et al., 2013).

Cells were cultured in high-glucose Dulbecco's modified Eagle's medium (DMEM, Life Technologies) supplemented with 10% fetal calf serum (FCS), 2 mM L-glutamine, 1 mM sodium pyruvate, and antibiotics. To block mitochondrial translation, 15 μg/ml doxycycline was added for six days to the culture medium. Cells were grown in exponential conditions and harvested at the indicated time points.

In vitro Import

Radiolabeled COX7A2L, COX6A and RISP proteins were obtained by coupled transcription and translation in the presence of ^{35}S-methionine (PerkinElmer) using TNT SP6 Quick Coupled System (Promega). Import experiments were performed on freshly isolated mitochondria from heart tissue as described before (Mourier et al., 2014a).

Immunoprecipitation

One milligram of mitochondrial protein from HEK293 transduced cells was solubilized in 600 μl of 4 g /g digitonin-to-protein buffer as for BNE analyses. After centrifugation for 30 min at 13,000 rpm at 4 °C, 50 μg of the supernatant was separated as the input fraction. The remainder supernatant was co-immunoprecipitated in resin spin columns (Pierce Co-IP Kit, Thermo Scientific) in which 15 μg of antibodies against DDK-tag (Oncogene), CORE2 or COX1 had been previously immobilized. The mixture was gently incubated overnight at 4°C in a rotating shaker and centrifuged at 1000 g for 1 min to separate the flow-through fraction. The column was washed three times with Lysis Buffer containing 1% NP-40 and proteins were eluted. The immunoprecipitate was divided into three aliquots, treated with 5× Loading Sample Buffer and heated at 95 °C for 5 minutes prior to loading.

Blue Native Electrophoresis and In-Gel Activity Assays

Mitochondrial pellets and blue native analyses were performed as described before (Moreno-Lastres et al., 2012; Mourier et al., 2014a). Native PAGE™ Novex® 3-12% Bis-Tris Protein Gels (Life Technologies) or self-made 4-10% polyacrylamide gradient gels were loaded with 60-80 μg of mitochondrial protein. After electrophoresis, proteins were transferred to nitrocellulose or PVDF membranes at 40 V overnight and probed with specific antibodies.

Antibodies

Western blot was performed using primary antibodies raised against COX7A2L (ProteinTech), Myc (Origene), turbo-GFP (Origene), HA (Roche), β-actin (Sigma), and against the following human OXPHOS subunits: NDUFS1 (GeneTex); NDUFA9, NDUFB8, CORE2, RISP, CYC1, UQCRB, UQCRQ, COX1, COX4, COX5A, COX6C, SDHA, SDHB (Mitosciences); and COX5B (Santa Cruz). Peroxidase-conjugated anti-mouse and anti-rabbit IgGs were used as secondary antibodies (Molecular Probes). Immunoreactive bands were detected with an ECL prime Western Blotting Detection Reagent (Amersham) in a ChemiDoc™ MP Imager (Biorad). Optical densities of the immunoreactive bands were measured using the ImageLab™ (Biorad) and ImageJ analysis softwares.

Indirect Immunofluorescence

Cells were fixed with 4% paraformaldehyde for 15 min, permeabilized for 15 min with 0.1% Triton X-100, and incubated in blocking buffer containing 10% goat serum for 1h. Cover slips were incubated with an antibody against monoclonal complex V α subunit and a Texas Red-conjugated anti-mouse secondary antibody (Abcam). Cover slips were rinsed, mounted in ProLong Gold antifade reagent (Molecular Probes) on glass slides, and cells were viewed with a Zeiss LSM 510 Meta confocal microscope and a 63× planapochromat oil inmersion objective (NA: 1.42). Sequential scanning of green and red channels was performed to avoid bleed-through effect. Cells were imaged randomly with 0,5-1,0 μm slices and 1024×1024 pixels resolution. For colocalization analysis, the “Merge channels” plugin from the ImageJ 1.48v software was used.

Statistical Data Analysis

All experiments were performed at least in triplicate and results were presented as mean ± standard deviation (SD) values. Statistical p values were obtained by application of the Friedman and Mann-Whitney U tests using the SPSS v21.0 program.

Ethics Statement

This study was performed in accordance with the guidelines of the Federation of European Laboratory Animal Science Associations. The protocol was approved by the Landesamt für Natur, Umwelt und Verbraucherschutz in Nordrhein-Westfalen in Germany.

Supplementary Material

Refer to Web version on PubMed Central for supplementary material.

Acknowledgments

Authors acknowledge Prof. Leo Nijtmans, Prof. Carlos Moraes and Prof. Giovanni Manfredi for kindly providing the mutant cybrids, and Prof. Antoni Barrientos and Prof. Flavia Fontanesi for manuscript revision and fruitful discussion. The proteomic analysis was carried out in the Proteomics Facility UCM-FPCM, a member of ProteoRed network (Spain). This work was funded by Instituto de Salud Carlos III (grant numbers PI11-00182 and PI14-00209 to C.U., PI12-01683 to M.A.M., and PI12-00933 to S.C.), by Comunidad Autónoma de Madrid (P2010/BMD-2361 to C.U. and P2010/BMD-2402 to M.A.M. and S.C.), by European FEDER Funds, by Association Française contre les Myopathies (16086) to E.F.V., by an European Research Council advanced investigator grant (268897) and grants from the Deutsche Forschungsgemeinschaft (SFB829) and the Swedish Research Council (2015-00418) to N.G.L., and by NIH-NIGMS (1R01GM105781-01) to C.U.

References

Acin-Perez R, Fernandez-Silva P, Peleato ML, Perez-Martos A, Enriquez JA. Respiratory active mitochondrial supercomplexes. Mol Cell. 2008; 32:529–539. [PubMed: 19026783]

Althoff T, Mills DJ, Popot JL, Kuhlbrandt W. Arrangement of electron transport chain components in bovine mitochondrial supercomplex I(1)III(2)IV(1). EMBO J. 2011; 30:4652–4664. [PubMed: 21909073]

Barrientos A, Ugalde C. I function, therefore I am: overcoming skepticism about mitochondrial supercomplexes. Cell Metab. 2013; 18:147–149. [PubMed: 23931749]

Bianchi C, Genova ML, Parenti Castelli G, Lenaz G. The mitochondrial respiratory chain is partially organized in a supercomplex assembly: kinetic evidence using flux control analysis. J Biol Chem. 2004; 279:36562–36569. [PubMed: 15205457]

Blaza JN, Serreli R, Jones AJ, Mohammed K, Hirst J. Kinetic evidence against partitioning of the ubiquinone pool and the catalytic relevance of respiratory-chain supercomplexes. Proc Natl Acad Sci USA. 2014; 111:15735–15740. [PubMed: 25331896]

Bruno C, Martinuzzi A, Tang Y, Andreu AL, Pallotti F, Bonilla E, Shanske S, Fu J, Sue CM, Angelini C, et al. A stop-codon mutation in the human mtDNA cytochrome c oxidase I gene disrupts the functional structure of complex IV. Am J Hum Genet. 1999; 65:611–620. [PubMed: 10441567]

Cruciat CM, Brunner S, Baumann F, Neupert W, Stuart RA. The cytochrome bc1 and cytochrome c oxidase complexes associate to form a single supracomplex in yeast mitochondria. J Biol Chem. 2000; 275:18093–18098. [PubMed: 10764779]

Chen YC, Taylor EB, Dephoure N, Heo JM, Tonhato A, Papandreou I, Nath N, Denko NC, Gygi SP, Rutter J. Identification of a protein mediating respiratory supercomplex stability. Cell Metab. 2012; 15:348–360. [PubMed: 22405070]

Desmurs M, Foti M, Raemy E, Vaz FM, Martinou JC, Bairoch A, Lane L. C11orf83, a mitochondrial cardiolipin-binding protein involved in bc1 complex assembly and supercomplex stabilization. Mol Cell Biol. 2015

Dudkina NV, Kudryashev M, Stahlberg H, Boekema EJ. Interaction of complexes I, III, and IV within the bovine respirasome by single particle cryoelectron tomography. Proc Natl Acad Sci USA. 2011; 108:15196–15200. [PubMed: 21876144]

Fernández-Vizarra E, Zeviani M. Nuclear gene mutations as the cause of mitochondrial complex III deficiency. Front Genet. 2015; 6:134. [PubMed: 25914718]

Hatle KM, Gummadidala P, Navasa N, Bernardo E, Dodge J, Silverstrim B, Fortner K, Burg E, Suratt BT, Hammer J, et al. MCJ/DnaJC15, an endogenous mitochondrial repressor of the respiratory chain that controls metabolic alterations. Mol Cell Biol. 2013; 33:2302–2314. [PubMed: 23530063]

Ikeda K, Shiba S, Horie-Inoue K, Shimokata K, Inoue S. A stabilizing factor for mitochondrial respiratory supercomplex assembly regulates energy metabolism in muscle. Nat Commun. 2013; 4:2147. [PubMed: 23857330]

Jha P, Wang X, Auwerx J. Analysis of mitochondrial respiratory chain supercomplexes using blue native polyacrylamide gel electrophoresis (BN-PAGE). Curr Protoc Mouse Biol. 2016; 6:1–14. [PubMed: 26928661]

Lapuente-Brun E, Moreno-Loshuertos R, Acin-Perez R, Latorre-Pellicer A, Colas C, Balsa E, Perales-Clemente E, Quiros PM, Calvo E, Rodriguez-Hernandez MA, et al. Supercomplex assembly determines electron flux in the mitochondrial electron transport chain. Science. 2013; 340:1567–1570. [PubMed: 23812712]

Maranzana E, Barbero G, Falasca AI, Lenaz G, Genova ML. Mitochondrial respiratory supercomplex association limits production of reactive oxygen species from complex I. Antioxid. Redox Signal. 2013; 19:1469–1480.

Milenkovic D, Matic S, Kuhl I, Ruzzenente B, Freyer C, Jemt E, Park CB, Falkenberg M, Larsson NG. TWINKLE is an essential mitochondrial helicase required for synthesis of nascent D-loop strands and complete mtDNA replication. Hum Mol Genet. 2013; 22:1983–1993. [PubMed: 23393161]

Moreno-Lastres D, Fontanesi F, Garcia-Consuegra I, Martin MA, Arenas J, Barrientos A, Ugalde C. Mitochondrial complex I plays an essential role in human respirasome assembly. Cell Metab. 2012; 15:324–335. [PubMed: 22342700]

Mourier A, Matic S, Ruzzenente B, Larsson NG, Milenkovic D. The Respiratory Chain Supercomplex Organization Is Independent of COX7a2l Isoforms. Cell Metab. 2014a; 20:1069–1075. [PubMed: 25470551]

Mourier A, Ruzzenente B, Brandt T, Kühlbrandt W, Larsson NG. Loss of LRPPRC causes ATP synthase deficiency. Hum Mol Genet. 2014b; 23:2580–2592. [PubMed: 24399447]

Müller CS, Bildl W, Haupt A, Ellenrieder L, Becker T, Hunte C, Fakler B, Schulte U. Cryo-slicing BN-MS - a novel technology for high-resolution complexome profiling. Mol Cell Proteomics. 2015

Rana M, de Coo I, Diaz F, Smeets H, Moraes CT. An out-of-frame cytochrome b gene deletion from a patient with parkinsonism is associated with impaired complex III assembly and an increase in free radical production. Ann Neurol. 2000; 48:774–781. [PubMed: 11079541]

Rigoulet M, Mourier A, Galinier A, Casteilla L, Devin A. Electron competition process in respiratory chain: regulatory mechanisms and physiological functions. Biochim Biophys Acta. 2010; 1797:671–677. [PubMed: 20117078]

Sánchez E, Lobo T, Fox JL, Zeviani M, Winge DR, Fernández-Vizarra E. LYRM7/MZM1L is a UQCRFS1 chaperone involved in the last steps of mitochondrial Complex III assembly in human cells. Biochim Biophys Acta. 2013; 1827:285–293. [PubMed: 23168492]

Schagger H, de Coo R, Bauer MF, Hofmann S, Godinot C, Brandt U. Significance of respirasomes for the assembly/stability of human respiratory chain complex I. J Biol Chem. 2004; 279:36349–36353. [PubMed: 15208329]

Schagger H, Pfeiffer K. Supercomplexes in the respiratory chains of yeast and mammalian mitochondria. EMBO J. 2000; 19:1777–1783. [PubMed: 10775262]

Smith PM, Fox JL, Winge DR. Biogenesis of the cytochrome bc(1) complex and role of assembly factors. Biochim Biophys Acta. 2012; 1817:872–882. [PubMed: 22564912]

Strogolova V, Furness A, Robb-McGrath M, Garlich J, Stuart RA. Rcf1 and Rcf2, members of the hypoxia-induced gene 1 protein family, are critical components of the mitochondrial cytochrome bc1-cytochrome c oxidase supercomplex. Mol Cell Biol. 2012; 32:1363–1373. [PubMed: 22310663]

Trouillard M, Meunier B, Rappaport F. Questioning the functional relevance of mitochondrial supercomplexes by time-resolved analysis of the respiratory chain. Proc Natl Acad Sci USA. 2011; 108:1027–1034.

Ugalde C, Hinttala R, Timal S, Smeets R, Rodenburg RJ, Uusimaa J, van Heuvel LP, Nijtmans LG, Majamaa K, Smeitink JA. Mutated ND2 impairs mitochondrial complex I assembly and leads to Leigh syndrome. Mol Genet Metab. 2007; 90:10–14. [PubMed: 16996290]

Vukotic M, Oeljeklaus S, Wiese S, Vogtle FN, Meisinger C, Meyer HE, Zieseniss A, Katschinski DM, Jans DC, Jakobs S, et al. Rcf1 mediates cytochrome oxidase assembly and respirasome formation, revealing heterogeneity of the enzyme complex. Cell Metab. 2012; 15:336–347. [PubMed: 22342701]

Highlights

1. COX7A2L preferentially interacts with respiratory chain complex III
2. COX7A2L is essential to stabilize the III_2+IV supercomplex
3. COX7A2L is not necessary for biogenesis or maintenance of the respirasome
4. Biogenesis of the III_2+IV supercomplex is not necessary for respirasome formation

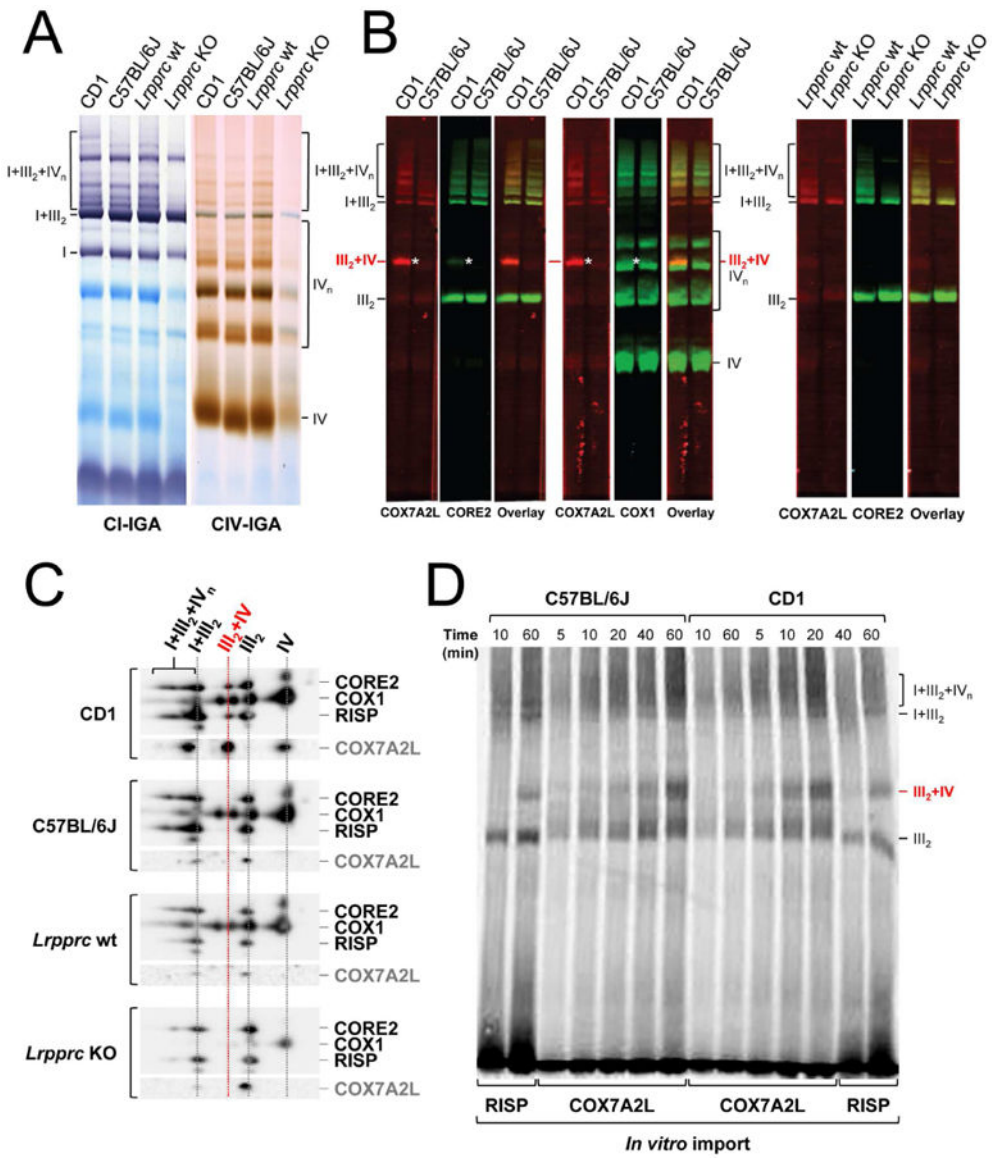

Figure 1. Mouse COX7A2L behaves as a complex III-binding protein specifically required for SC III_2+IV assembly

(A) Supramolecular organization of the respiratory chain in heart mitochondria from wild-type CD1, C57BL/6J and C57BL/6N (*Lrpprc* wt) mouse strains, as well as from *Lrpprc* deficient mice with a C57BL/6N genetic background. Mitochondria were extracted with a digitonin:protein ratio of 4 g/g and analyzed by BN-PAGE followed by CI and CIV-IGA assays. **(B)** Heart mitochondria were extracted with a digitonin:protein ratio of 6 g/g and analyzed by BN-PAGE followed by western blot with double fluorescent detection of CIII and CIV (anti-CORE2 or anti-COX1, green color) and COX7A2L-containing complexes (anti-COX7A2L, red color). White asterisks show the localization of SC III_2+IV. **(C)** Heart mitochondria were extracted with a digitonin:protein ratio of 4 g/g and analyzed by 2D-BN/SDS-PAGE followed by western blot and immunodetection with antibodies against COX7A2L and the indicated OXPHOS subunits. **(D)** Import of radiolabeled RISP and COX7A2L precursors and subsequent incorporation into CIII and SCs in intact heart

mitochondria from C57BL/6J and CD1 mouse strains. After the indicated incubation times (in minutes), mitochondria were solubilized in 6 g/g digitonin per protein and analyzed by BN-PAGE. I+III_2+IV_n, SC containing CI, CIII and CIV. I+III_2, SC containing CI and CIII. III_2+IV, SC containing CIII and CIV. III_2, complex III dimer; IV, free complex IV; IV_n, complex IV oligomers. See also Figure S1.

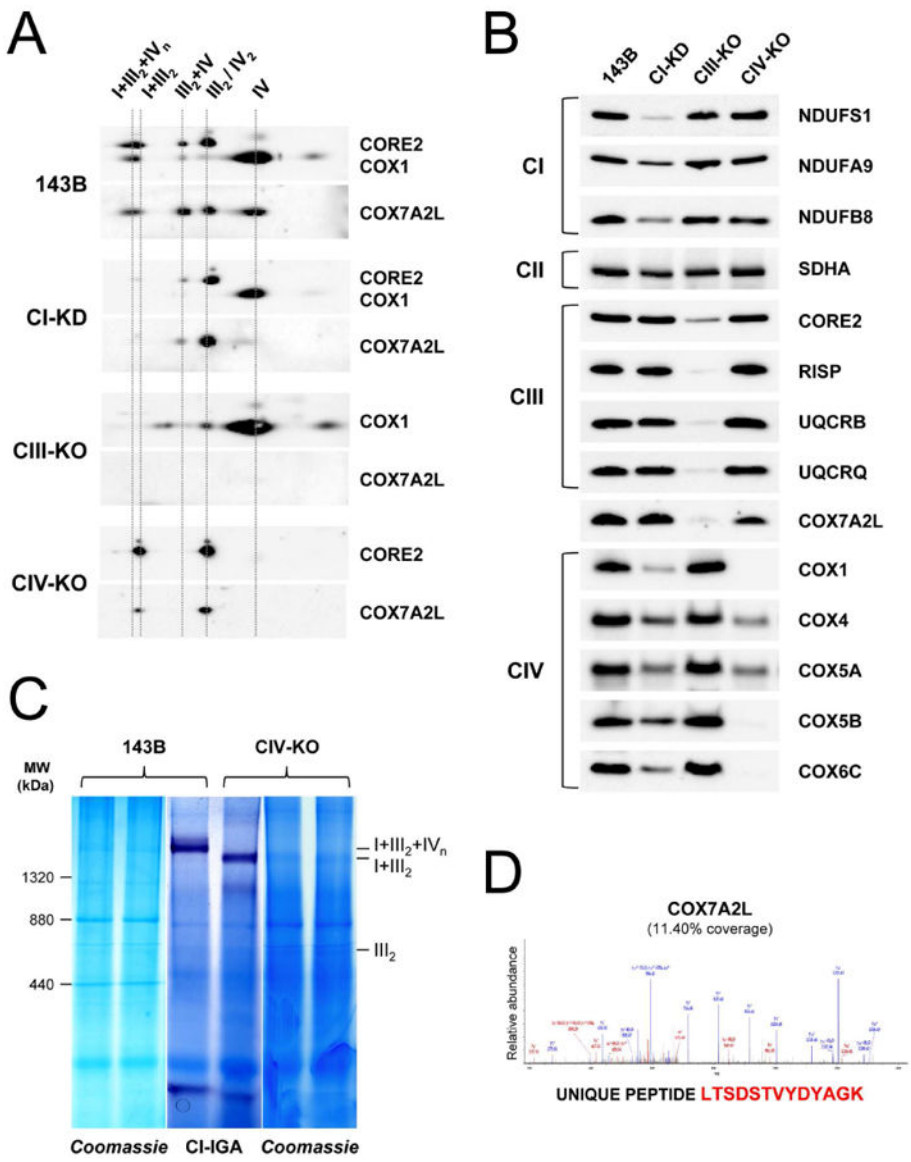

Figure 2. Human COX7A2L comigrates with respiratory chain supercomplexes and free complexes III and IV

(A) Mitochondria from control 143B cells and mutant cybrids defective in complexes I (CI-KD), III (CIII-KO) and IV (CIV-KO) were extracted with a digitonin:protein ratio of 4 g/g and analyzed by 2D-BN/SDS-PAGE and western blot with antibodies raised against COX7A2L, CORE2 and COX1. **(B)** Mitochondrial lysates from control and mutant cybrids were analyzed by SDS- PAGE and western blot with the indicated antibodies. **(C)** BN-PAGE and CI-IGA analysis of control 143B cells and CIV-KO mutant cybrids. After Coomassie staining, the SC I+III_2+IV_1 band was excised from the control lane and the bands corresponding to SC I+III_2 and CIII were excised from the CIV-KO lane. Bands were subsequently analyzed by liquid chromatography coupled to tandem mass spectrometry. **(D)** MS/MS spectra from the doubly-charged COX7A2L tryptic peptide unambiguously detected by LC-ESI/MS in two independent experiments per sample. The amino acid sequence of the identified COX7A2L unique peptide is highlighted in red. The most intense signals on the

MS/MS spectra correspond to the main fragmentation series (b-amino and y-carboxy). Doubly-charged fragments are marked with superscript 2+. I+III_2+IV_n, SC containing CI, CIII and CIV. I+III_2, SC containing CI and CIII. III_2+IV, SC containing CIII and CIV. III_2, complex III dimer. IV, complex IV. IV_2, complex IV dimer. See also Table S1 and Figure S2.

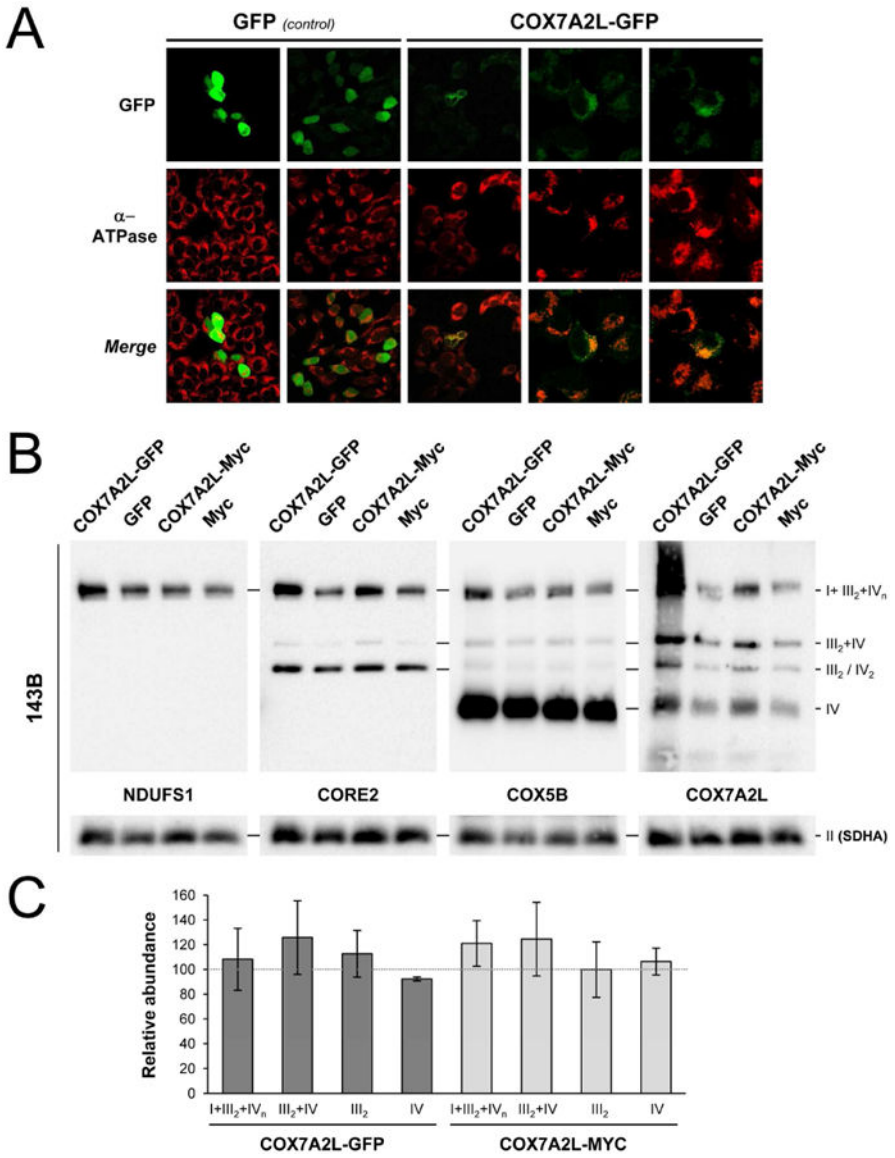

Figure 3. Overexpressed COX7A2L localizes to mitochondria with minor effects on the respiratory chain complexes and supercomplexes

(A) Confocal microscopy of 143B cells transiently transfected with the COX7A2L-GFP construct and with the empty-GFP vector as a control. Upper images show the GFP signal. Middle images show the mitochondrial network using an antibody against the ATPase a subunit. Lower images show the overlay between the two signals. **(B)** BN-PAGE and western-blot analyses of control 143B cells transiently transfected both with the COX7A2L-GFP or COX7A2L-MYC-DDK constructs, and with their corresponding empty vectors. Membranes were incubated with antibodies raised against COX7A2L and the indicated OXPHOS subunits. **(C)** Densitometric analysis of the MRC complexes and SCs in 143B cells transfected with both COX7A2L- tagged constructs. The optical densities of immunoreactive bands that had not reached saturation levels were measured with the ChemiDoc™ MP Image Analyzer software package (Biorad). The antibody signals within the same structures were quantified; the mean values were normalized by CII and expressed

as percentages of the cells transfected with the empty vectors (horizontal bar). Values represent the mean ± SD from four independent experiments. $I+III_2+IV_n$, SC containing CI, CIII and CIV. III_2+IV, SC containing CIII and CIV. III_2, complex III dimer. IV, complex IV. IV_2, complex IV dimer. II, complex II. See also Figure S3.

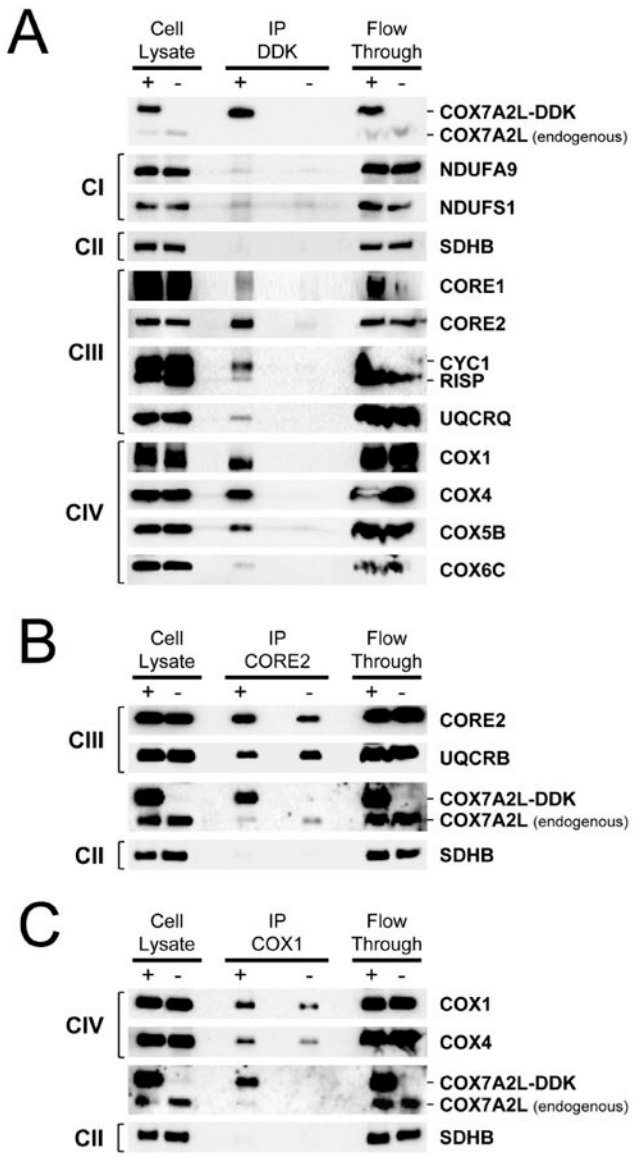

Figure 4. COX7A2L physically binds complexes III and IV

(A) COX7A2L co-immunoprecipitation assay. Digitonin-solubilized mitochondrial extracts (4 g digitonin / g protein) from HEK293 cells transiently transfected with COX7A2L-MYC-DDK (+) or the empty MYC-DDK construct (-) were immunoprecipitated using an anti-DDK antibody. **(B)** The same digitonin-solubilized mitochondrial extracts were immunoprecipitated using antibodies against CORE2, or **(C)** against COX1. Samples were subsequently analyzed by SDS-PAGE and western blot with the indicated antibodies.

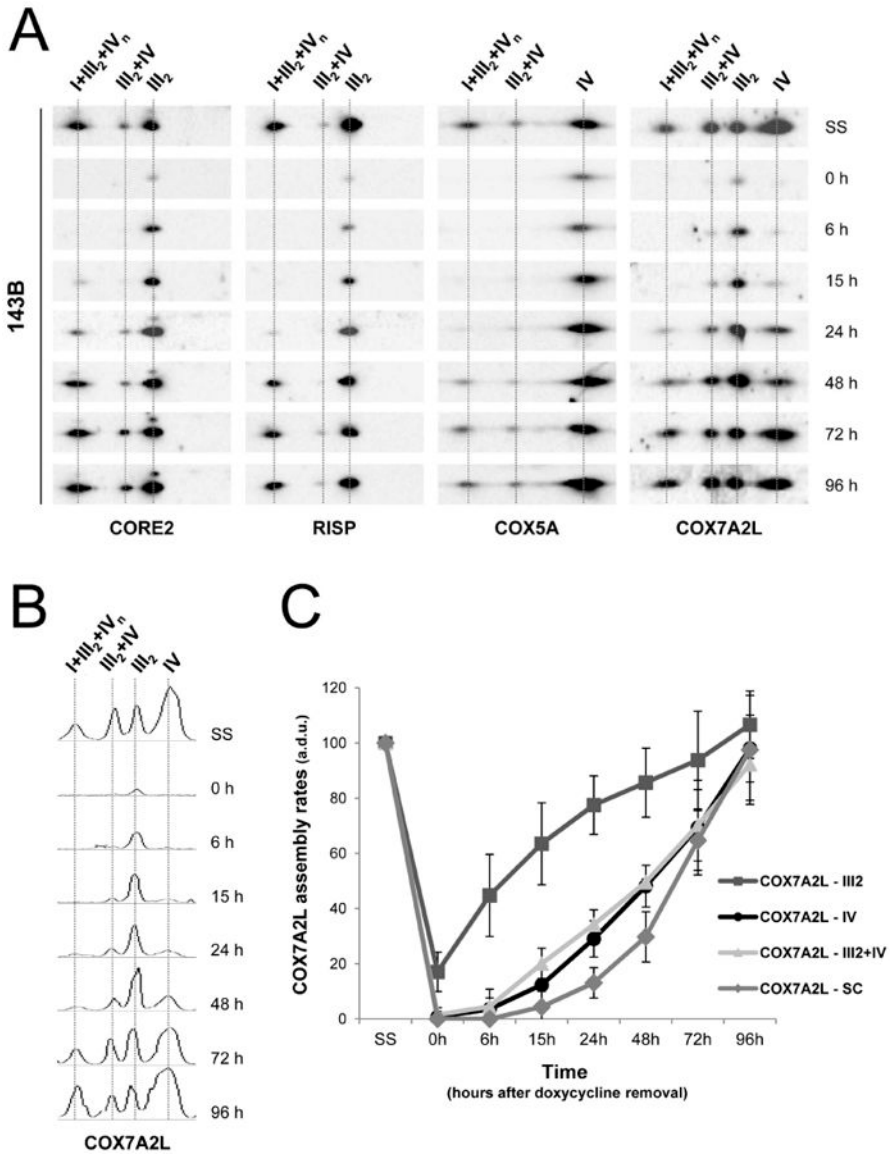

Figure 5. Assembly kinetics of COX7A2L in free complexes and supercomplexes

(A) Mitochondria from doxycycline-treated 143B cells were extracted with a digitonin:protein ratio of 4 g/g and analyzed by 2D-BN/SDS-PAGE and western blot with the indicated antibodies. **(B)** Densitometric profiles representing the assembly progress of COX7A2L in CIII- and CIV- containing structures. (**C)** Mean incorporation rates of COX7A2L into CIII- and CIV- containing structures. The signals from three independent experiments were quantified and normalized by CII. Time point values are expressed as percentages of the untreated cells (SS), and indicated as means ± SD. $I+III_2+IV_n$, SC containing CI, CIII and CIV. III_2+IV, SC containing CIII and CIV. III_2, complex III dimer. IV, complex IV. See also Figure S4.

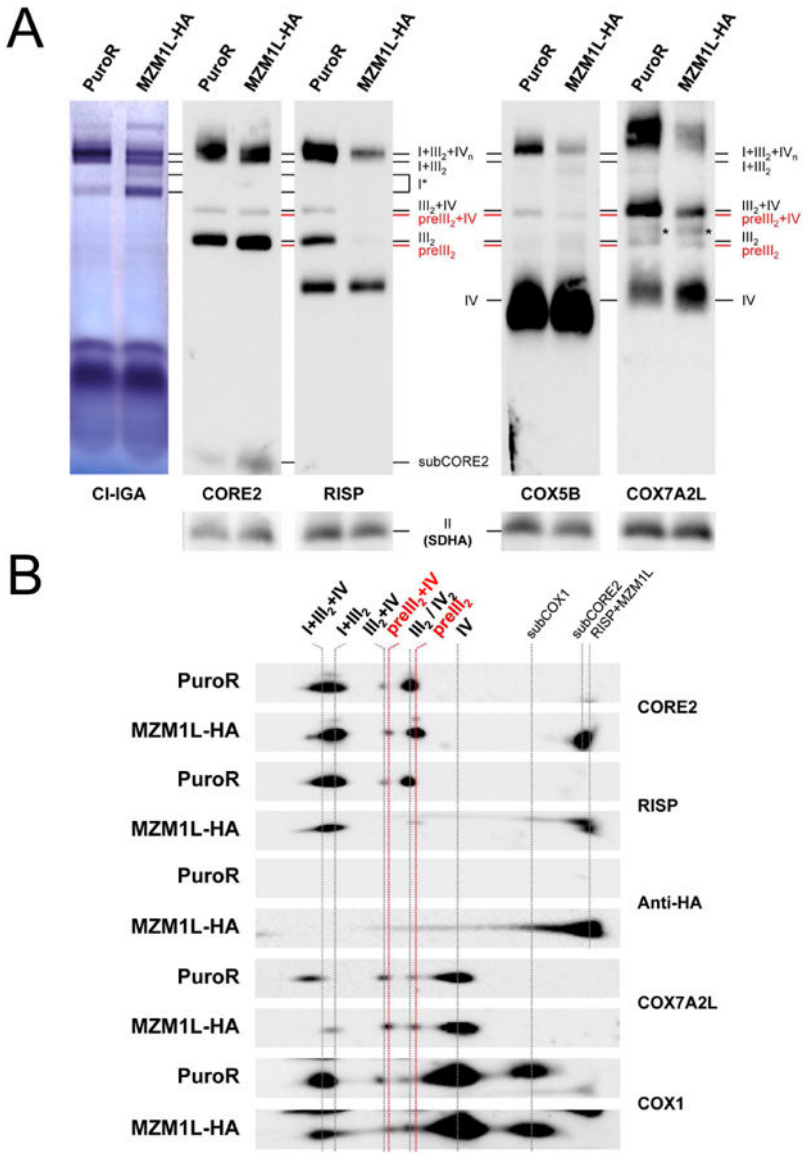

Figure 6. COX7A2L binds to complex III assembly intermediates

(A) Digitonin-solubilized mitochondrial extracts (4 g digitonin / g protein) from HeLa cells transduced with the MZM1L-HA contruct or with the empty vector (PuroR) were analyzed by BN-PAGE and CI-IGA assays or alternatively, by western blot and immunodetection. Asterisks indicate unspecific signals that do not appear on 2D-BN/SDS-PAGE gels. **(B)** Subsequent 2D-BN/SDS-PAGE and western blot analyses were performed with antibodies against COX7A2L, the indicated OXPHOS subunits and the HA epitope. $I+III_2+IV_n$, SC containing CI, CIII and CIV. $I+III_2$, SC containing CI and CIII. I*, complex I-containing structure. III_2+IV, SC containing CIII and CIV. Pre-III_2+IV, SC containing pre-CIII and CIV. III_2, complex III dimer. Pre-III_2, pre-CIII lacking the RISP subunit. IV, complex IV; IV_2, complex IV dimer. II, complex II. Subcomplexes that contain CORE2 and COX1 are indicated as subCORE2 and subCOX1, respectively. The association of RISP and MZM1L is indicated as RISP+MZM1L.

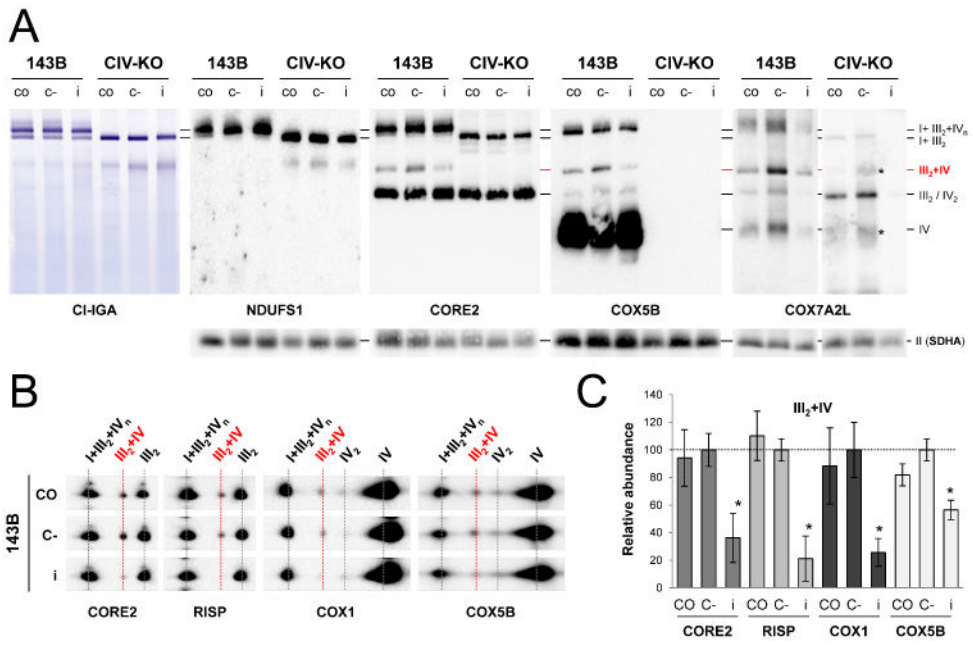

Figure 7. COX7A2L down regulation specifically decreases the levels of supercomplex III_2+IV without affecting respirasome biogenesis

The effect of COX7A2L knockdown on MRC complex assembly was investigated in untreated (CO), mock-transfected (C-), and *COX7A2L* siRNA-transfected (i) 143B cells and in the CIV-KO mutants. **(A)** Mitochondria were extracted with a digitonin:protein ratio of 4 g/g and analyzed by BN-PAGE followed by CI-IGA assays, or alternatively, by western blot and immunodetection with the indicated antibodies. **(B)** 2D-BN/SDS-PAGE and western blot analyses of 143B cells upon *COX7A2L* silencing. **(C)** The optical densities of immunoreactive bands that had not reached saturation levels were measured. The signals within SC III_2+IV were quantified, normalized by CII, and shown as means ± SD from five independent siRNA experiments. Values are expressed as percentages of the cells transfected with scramble RNA (C-, horizontal bar). I+III_2+IV_n, SC containing CI, CIII and CIV. I+III_2, SC containing CI and CIII. III_2+IV, SC containing CIII and CIV. III_2, complex III dimer. IV, complex IV. IV_2, complex IV dimer. II, complex II. See also Figures S5 and S6.